Lattice location and electrical conductivity in Sb-implanted rutile

I. Khubeis,* R. Fromknecht, and O. Meyer
Forschungszentrum Karlsruhe, Institut für Nukleare Festkörperphysik, P.O. Box 36 40, D-76021 Karlsruhe, Germany
(Received 3 September 1996)

Single crystals of TiO_2 (rutile) were implanted with Sb ions applying fluences of $2\times10^{13}/cm^2$ to $5\times10^{16}/cm^2$ at 300 keV. The lattice location together with the ion range and damage distribution was measured using Rutherford-backscattering and channeling. The conductivity was measured as a function of temperature in the region between 6 and 300 K. Up to a dose of $5\times10^{15}/cm^2$ the Sb atoms were entirely substitutional on Ti sites as concluded from channeling measurements on $\langle001\rangle$- and $\langle100\rangle$-oriented TiO_2 single crystals. A large increase of the conductivity σ was observed with increasing Sb dose, indicating a saturation behavior at about 30 $\Omega^{-1}\,cm^{-1}$. Between 40 and 293 K $\ln\sigma$ was proportional to $T^{-1/2}$ for low doses, and proportional to $T^{-1/4}$ for doses of 1×10^{16} Sb/cm^2 and above, indicating that the transport mechanism is due to variable range hopping. [S0163-1829(97)02502-2]

I. INTRODUCTION

Ion implantation into TiO_2 revealed that various ions occupy substitutional sites by replacing Ti atoms.[1] The replacement of Ti atoms depends in a first approximation on the size mismatch energy of the implanted ions. A summary of all results obtained up till now was given recently[1] where it was shown that atoms with an atomic radii difference of $\Delta r=|r^i-r^{\mathrm{Ti}}|$ up to about 0.02 nm are highly substitutional. With increasing Δr the substitutional component decreased rapidly being zero for Δr values of 0.04, e.g., for La.[2] The maximum concentration of implanted ions on Ti sites may exceed that obtained by conventional doping.[3] Thus it is of interest if enhanced electrical doping may be obtained by ion implantation. The electrical conductivity of TiO_2, σ, increases by many orders of magnitude due to radiation damage.[4,5] Thus the influence of disorder and doping on σ have to be separated. It was shown that the increase of σ by disorder saturated with fluence at about 1 Ω^{-1} cm^{-1} for Kr (Ref. 4) and at about 0.3 Ω^{-1} cm^{-1} for Ar implantation.[5] Conductivity values which are larger than these values are generally attributed to the doping action of the implanted species. The next important question concerns the relation between lattice site occupation, possible charge state, and electrical conductivity. Here compensation as well as precipitation effects have to be considered. For Nb implanted into TiO_2 it is assumed that the pentavalent charge state is compensated by defects such as Ti^{3+}, while for Nb doses greater than $1\times10^{17}/cm^2$ electron hopping between Nb and Ti precipitates may occur as charge-transport processes.[6] Implantation of Sn which is substitutional up to concentrations of about 1 at. % leads to an unexpected increase of 5–30 $\Omega^{-1}\,cm^{-1}$, which is higher than conductivity values of about 1 $\Omega^{-1}\,cm^{-1}$, obtained by conventional doping.[3] This rather high σ value obtained by Sn doping is not well understood as the most probable charge state of Sn is 4^+, equal to that of Ti in TiO_2. Therefore it was of interest to study the lattice site occupation and the conductivity of Sb implanted into TiO_2. For Sb a charge state of 5 is possible and the results may then be compared with those of Nb, which is the most effective dopant found up till now in TiO_2 using ion implantation.[6]

II. EXPERIMENT

Polished single-crystal TiO_2 slices of $\langle100\rangle$ and $\langle001\rangle$ orientation as obtained from the manufacturer were used for our experiments. Ion implantation was performed at room temperature and at 77 K using a Danfysik ion implanter. 300 keV Sb ions in the fluence region between $2\times10^{13}/cm^2$ and $5\times10^{16}/cm^2$ were used. He ions of 2 MeV were generated by a Van de Graaff accelerator and applied *in situ* for Rutherford-backscattering and channeling (RBS-C) studies to determine the damage and ion distribution and the lattice location. The ion range and damage distribution were evaluated and compared with results of the TRIM program.[7] The displacement energies used were 50 eV for both Ti and O.[8]

Random, $\langle001\rangle$- and $\langle100\rangle$-aligned backscattering spectra were measured after Sb ion implantation and after annealing when the sample was cooled to room temperature. In some cases the backscattering spectra were measured as a function of the tilt angle through the $\langle001\rangle$ and $\langle001\rangle$ crystal directions, choosing tilt planes with respect to crystal planes. Energy windows can then be selected freely in the Ti damage peak area, at energies below the damage peak, and in the impurity region in order to determine the relative backscattering yields in dependence on the tilt angle. Such angular scans are characterized by the minimum yield $X_{\min}$, which is the yield obtained for perfect alignment of the incident beam with crystal direction normalized to the yield for random incidence, and the critical angle $\Psi_{1/2}$, which is half of the tilt angle at half maximum of the angular yield curve. The apparent substitutional fraction f_s is defined as

$$f_s=(1-X^i_{\min})/(1-X^h_{\min})\,. \tag{1}$$

$X^i_{\min}$ is defined as $A^{\mathrm{Sb}}{}_{\mathrm{al}}/A^{\mathrm{Sb}}{}_r$ where $A^{\mathrm{Sb}}{}_{\mathrm{al}}$ and $A^{\mathrm{Sb}}{}_r$ are the Sb peak areas of the aligned and the random spectra, respectively. $X^h{}_{\min}$ is the ratio of the aligned and random yield of Ti at a depth where the Sb atoms are located. This formula is

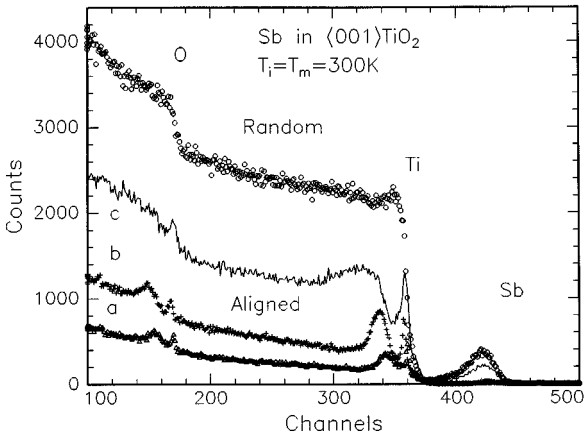

FIG. 1. Random and ⟨001⟩-aligned backscattering spectra as a function of ion fluence: 5×10^{14} (a), 1.5×10^{15} (b), 5×10^{15} Sb^+/cm^2 (c).

valid only if the ratio $\Psi^i_{1/2}/\Psi^h_{1/2}$ is close to unity and if the nonsubstitutional impurity atoms occupy random lattice positions.

The electrical conductivities were determined by applying a four-point probe with Au contacts sputtered through a mask onto the implanted area. The resistance was measured by a Keithley 617 electrometer using a current $I=1$ μA. The sample holder was inserted in a liquid-He-cooled cryostat which allows automated temperature-dependent measurements. The resistance $R=U/I$ is converted into a resistivity value ρ by $\rho=(U\pi d)/(I\ln 2)$, where d is the thickness of the implanted region. Assuming that ion doping plays the main role for the conductivity change, the half width at half maximum of the ion distribution is used, and d is equal to $2.35\times\Delta R_p$ ($\Delta R_p=$ range straggling).

III. RESULTS

A. Lattice disorder

Typical energy spectra of backscattered He ions for random and aligned incidence from ⟨001⟩- and ⟨100⟩-oriented TiO_2 single crystals are shown in Figs. 1 and 2, respectively. The Sb yield is energetically well separated from the Ti yield. From the Sb peak areas of the random and aligned spectra using Eq. (1) a substitutional fraction of 0.96 is obtained. The lattice location of Sb in TiO_2 is presented in more detail below. Two well-resolved damage peaks are seen for both the Ti and the O sublattices in the ⟨100⟩ and ⟨001⟩ crystalline direction. It is noted that in ⟨100⟩ direction the damage peak grows faster with ion fluence with respect to the surface peak as in ⟨001⟩ direction. Further it is seen that for a similar implanted ion dose the damage peak and the dechanneling is higher in the ⟨100⟩ direction. Those effects are attributed to the comparatively low steering force along ⟨100⟩, which is due to the fact that the distance between the Ti atoms along ⟨100⟩ is 1.6 times larger than that along ⟨001⟩. Similar features have been observed and discussed previously for Hg-implanted TiO_2 single crystals.[9] Multiple Gaussian and Lorentz fit peak area analysis was only performed for low dose implants, where the damage and the surface peaks are well separated for both sublattices.

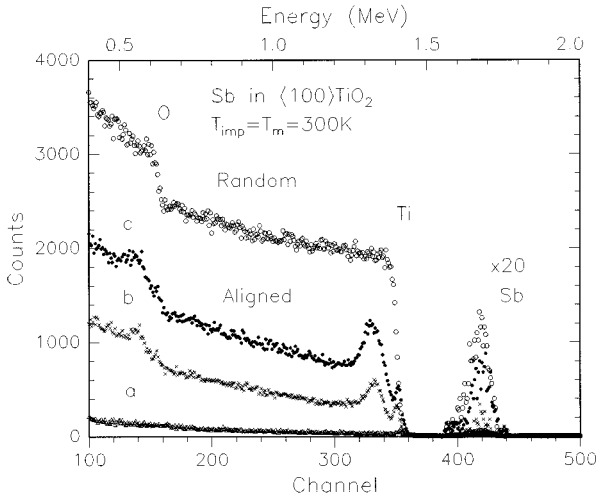

FIG. 2. Random and ⟨100⟩-aligned backscattering spectra for the virgin sample (a) and at ion fluences of 5×10^{14} Sb^+/cm^2 (b) and 1×10^{15} Sb^+/cm^2 (c).

For the Ti to O peak area ratios nearly stochiometric values of 0.50 ± 0.05 where obtained for the damage as well as for the surface peaks. The latter result indicates that enhanced oxygen depletion due to preferential oxygen sputtering cannot be observed within the experimental accuracy. This is in agreement with previous results.[9]

Annealing experiments have been performed using the amorphous rutile phase as well as the partly damaged rutile phase. The amorphous phase was produced by implanting 5×10^{14} Sb/cm^2 into TiO_2 at 77 K. The sample was then annealed to RT and further in air for 1 h at each temperature step in steps of 50 °C. Some ⟨001⟩-aligned spectra as a function of the annealing temperature are shown in Fig. 3. The disorder peak reaches the random level after implantation at 77 K and no change has been seen after annealing to 300 K. A small reduction of the width and the height of the disorder peak was first noted at 550 K. Up to 700 K no further change by

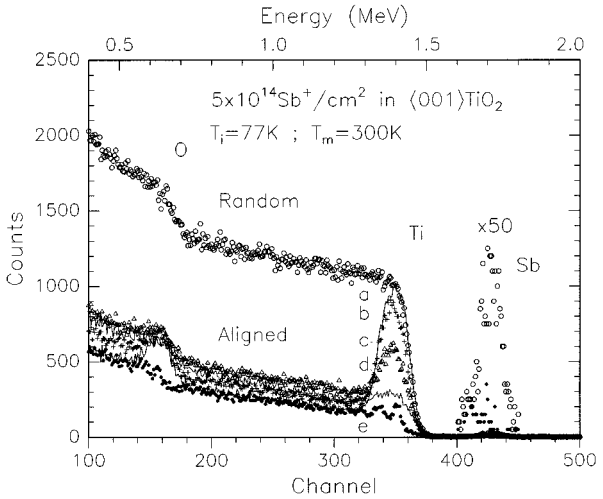

FIG. 3. Random and ⟨001⟩-aligned backscattering spectra from TiO_2 single crystals implanted with 5×10^{14} Sb^+/cm^2 at 77 K shown after annealing at 300 K (a), 600 K (b), 800 K (c), 900 K (d), and 1000 K (e).

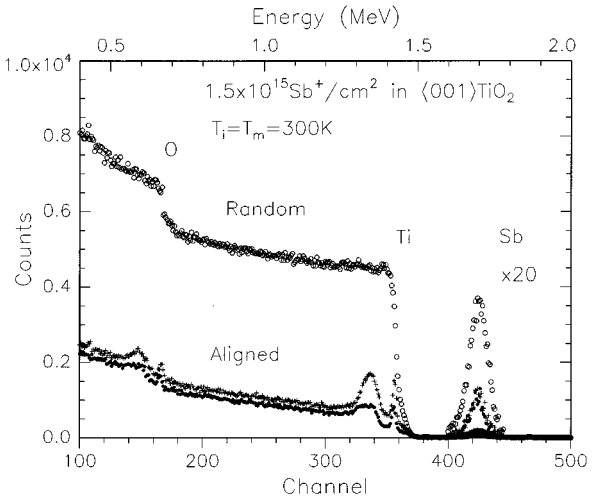

FIG. 4. Random and ⟨001⟩-aligned backscattering spectra from a TiO_2 single crystal implanted with 1.5×10^{15} Sb^+/cm^2 (a) and after annealing at 700 K for 1 h in air (b).

annealing was observed. A strong decrease of the disorder peak started at 800 K, and at 1000 K most of the disorder was annealed. A double-peak structure is noted after annealing at 1000 K consisting of a surface peak and a disorder peak. This damage distribution is similar to that obtained after low dose implantation shown in Fig. 1. The existence of two annealing stages at 550 and above 800 K is in agreement with previous results. However, the annealing process is different as previously the main damage started to anneal from the rear edge indicating solid phase epitaxial regrowth,[9,10] which is not the case here. Sb outdiffusion was not observed up to 1000 K and Sb reveals a high substitutional fraction (see below).

In contrast to the annealing behavior of the amorphous phase, the recovery of the partly damaged rutile phase is different at least in two respects. Previously it was shown that there is a strong recovery stage below 300 K.[9] Here it is demonstrated that in contrast to the amorphous phase the damaged rutile phase reveals an enhanced recovery also at 700 K. This is shown in Fig. 4, where the ⟨001⟩-aligned backscattering spectra are presented after implantation of 1.5×10^{15} Sb^+/cm^2 at 300 K and after annealing at 700 K in air for 1 h. It is seen that especially the Ti damage and surface peak areas are strongly reduced. Peak area analysis reveals that the Ti damage and surface peak areas were diminished by a factor of 2.2, while the oxygen damage and surface peak areas were reduced by a factor of 1.2 only, which indicates an enhanced defect level in the oxygen sublattice.

B. Lattice location of the Sb atoms

From the Sb peak areas, which are different for the random and aligned spectra as shown in Figs. 1–4, high substitutional fraction in the order of $f_s \approx 0.96$ are obtained using Eq. (1). In order to investigate the lattice location in more detail, angular scan measurements were performed through the ⟨001⟩ and ⟨100⟩ crystalline directions of TiO_2 single crystals, implanted with Sb ions in the fluence region of 2×10^{13} Sb/cm^2 to 5×10^{15} Sb/cm^2. A low dose of

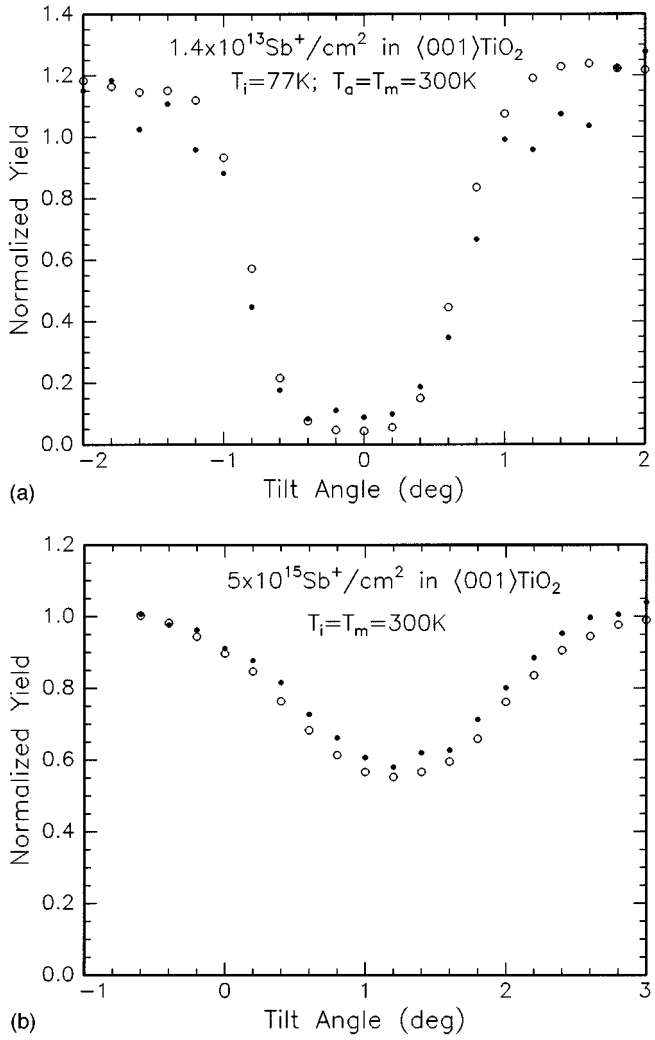

FIG. 5. Axial channeling scans through the ⟨001⟩ crystalline direction of TiO_2 single crystals implanted with 1.4×10^{13} Sb^+/cm^2 (a) and 5×10^{15} Sb^+/cm^2 (b).

2×10^{13} Sb^+/cm^2 was implanted at 77 K and was measured *in situ*. From the peak area ratios a f_s value of 0.96 was obtained. The sample was then annealed to 300 K and a strong annealing of the disorder was noted in agreement with previous observations.[9] Angular scan curves were measured at 300 K and are shown in Fig. 5(a). The angular-dependent Ti yield from an energy window in the Ti damage peak area and that of the Sb peak area nearly overlap in width and depth, indicating that Sb is located on Ti lattice sites. The angular width from an energy window of the oxygen damage peak is much smaller (not shown) which excludes the possibility that Sb is located on oxygen lattice sites. With increasing dose, nearly all Sb atoms occupy Ti lattice sites as is demonstrated in Fig. 5(b) for a dose of 5×10^{15} Sb^+/cm^2. Here the critical angle of the Sb dip (0.75 °) is slightly narrower than that of the Ti dip (0.80°), which may indicate a larger vibrational amplitude of Sb or rather small Sb displacements from the substitutional site in the order of 0.005 nm. With further increasing the Sb dose the radiation damage reaching the random level limits the application of the RBS-C technique.

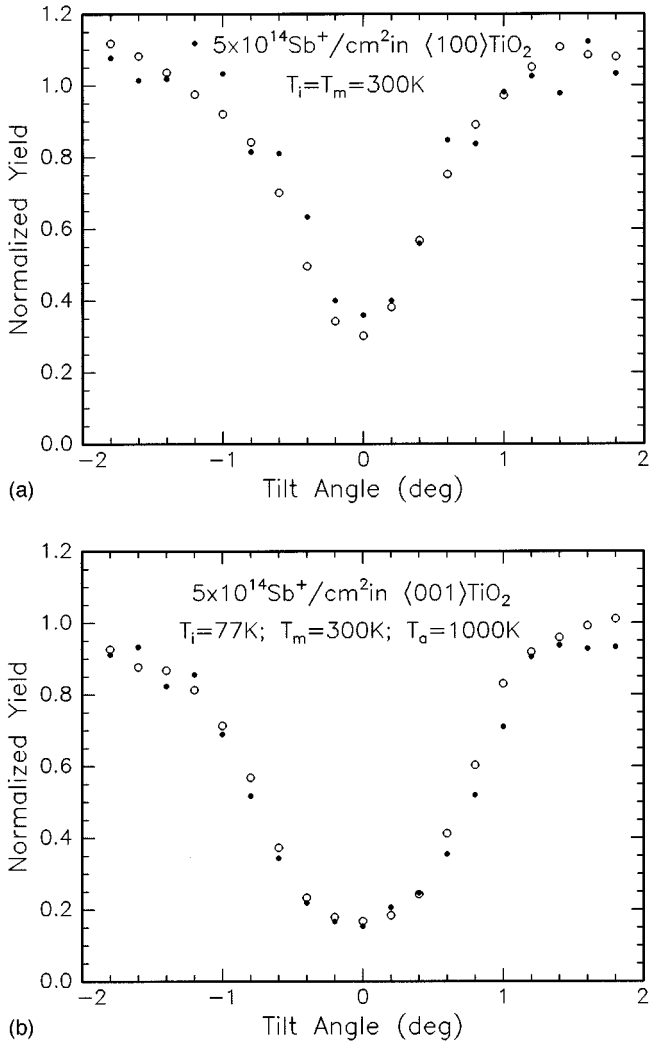

FIG. 6. Axial channeling scans of ⟨100⟩- and ⟨001⟩-oriented TiO_2 single crystals implanted with 5×10^{14} Sb^+/cm^2 (a) and 5×10^{14} Sb^+/cm^2 after annealing at 1000 K (b).

For the determination of the lattice location in crystals with noncubic symmetry it is necessary to perform channeling studies at least in two perpendicular directions. For example it was shown previously for In implanted in TiO_2, that with increasing the dose a fraction of In was displaced along the *c* axis. Such displacements can only be detected by channeling perpendicular to the *c* axis.[11]

Angular scan measurements have therefore been performed through the ⟨100⟩ axes of TiO_2 single crystals implanted with 6×10^{14} Sb^+/cm^2 and 1×10^{15} Sb^+/cm^2. The dip curves for Ti and Sb of the high dose implant are presented in Fig. 6(a). Due to the reduced steering force along ⟨100⟩ the critical angles are about 25% narrower than those through the ⟨001⟩ crystalline direction. The critical angles of Sb and Ti are nearly equal, supporting the result that Sb is substitutional up to a dose of 1×10^{15} Sb^+/cm^2.

Annealing of an amorphous layer at 1000 K leads to a large recovery of defects and to the incorporation of the implanted Sb atoms on Ti lattice sites. This is demonstrated in Fig. 6(b). From the nearly perfect overlap of the Ti and Sb scan curves it can be concluded that Sb is substitutional and not coherently precipitated where the $\Psi_{1/2}$ values would differ. From the unchanged peak area it can further be concluded that Sb does not reveal any diffusion up to 1000 K.

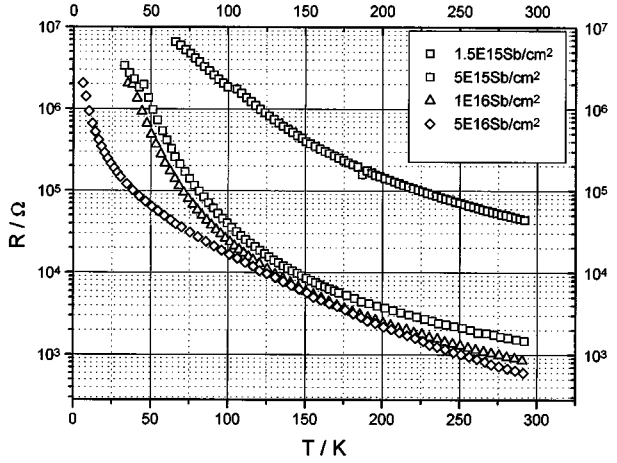

FIG. 7. Electrical conductance of Sb-implanted TiO_2 single crystals as function of *T*, with the fluence as a parameter.

C. Electrical conductivity measurements

The electrical resistance was measured as a function of temperature with the implanted Sb dose as parameter. The results are shown in Fig. 7 where ln*R* is plotted versus temperature. The resistance at room temperature decreases steeply with ion dose between $1.5\times10^{15}/cm^2$ and $5\times10^{15}/cm^2$ and approaches a saturation value of about 600 Ω at 5×10^{16} Sb/cm^2. This corresponds to a σ value of 31 $\Omega^{-1}cm^{-1}$ applying the measured width at half height of the Sb peak (see Fig. 1) as the thickness of the conducting sheet. From this value a range straggling, $\Delta R_p = 50$ nm is obtained, which is in good agreement with theory (45 nm). The room-temperature σ value is in good agreement with that previously observed for Sn implanted into TiO_2 (~30 Ω^{-1} cm^{-1}) and is two orders of magnitude higher than the saturation value for defect doping (0.3 $\Omega^{-1}cm^{-1}$).[5] The resistance increases with decreasing temperature indicating activated conduction (Fig. 7). The high dose sample reveals a reduced resistivity at low temperature, which might reflect the onset of a different additional transport mechanism.

In order to get more information on the transport mechanisms, the logarithm of the conductance was analyzed as a function of T^{-1}, $T^{-1/2}$, and $T^{-1/4}$. We found that the Arrhenius plot ($\ln\sigma\sim T^{-1}$) was not able to describe the data. The best fitting for the low dose samples ($1.5\times10^{15}/cm^2$ and $5\times10^{15}/cm^2$) was obtained by plotting $\ln G\sim T^{-1/2}$, as is shown in Fig. 8. For the high dose sample ($1\times10^{16}/cm^2$) a slightly better fit was obtained for $\ln\sigma\sim T^{-1/4}$. The electrical conductivity of the highest dose implant (5×10^{16} Sb/cm^2) can no longer be described by a single transport process over the total temperature region. The high-temperature region ($120\ K<T<300\ K$) as well as the low-temperature region ($6K<T<42$ K) can be fitted by plotting $\ln\sigma\sim T^{-1/4}$. In general the results indicate that the electron transport is due to hopping conduction, which is in agreement with previous studies.[5]

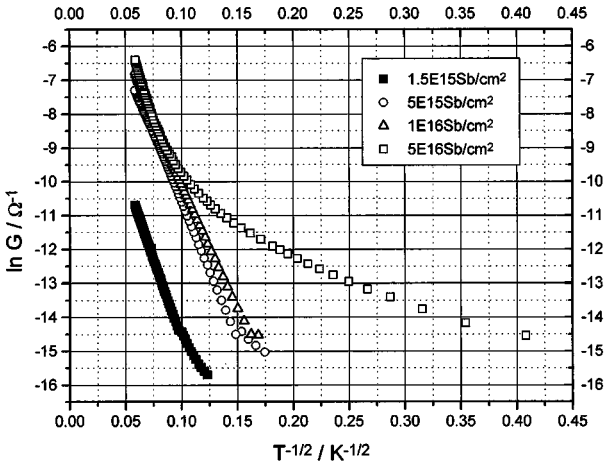

FIG. 8. Logarithm of the electrical conductance of Sb-implanted TiO_2 single crystals versus $T^{-1/2}$, with the fluence as a parameter.

IV. DISCUSSION AND CONCLUSIONS

The relation between lattice site occupation, charge state, and electrical conductivity in ion-implanted rutile cannot be evaluated without considering the large influence of defects on the electrical conductivity. Oxygen vacancies for example are known to increase the conductivity of TiO_{2-x} by many orders of magnitude up to values of about $1\,\Omega^{-1}\,\mathrm{cm}^{-1}$.[12] Therefore it is not astonishing that defects produced by noble-gas ion implantation cause a large increase in the conductivity with ion fluence up to saturation values of 0.3 $\Omega^{-1}\,\mathrm{cm}^{-1}$ for Ar in the disordered rutile phase and about 1 $\Omega^{-1}\,\mathrm{cm}^{-1}$ in the polycrystalline Ti_2O_3 phase which was formed by prolonged bombardment with Kr ions due to preferential oxygen sputtering.[4] Here we observed the displacement of Ti and O atoms in stoichiometric amounts also for the surface peak which excludes preferential oxygen sputtering as a means to produce phase transformation. This is in agreement with our previous observations on Hg in TiO_2, where the double-peak structure of the damage distribution was studied in more detail.[9] There we could exclude long-range atomic migration and pinning at the surface as well as changes of the composition by preferential oxygen sputtering as sources of surface damage peak formation.

The damage in the disordered rutile phase can readily be annealed in agreement with previous observations where annealing stages even below 300 K were found.[9] This is to be contrasted to the amorphous phase annealing where a first stage of a partial recovery is observed near 500–600 K, while the main damage recovery occurs at 900 K and above. During annealing of the amorphous phase Sb is incorporated on Ti lattice sites and no outdiffusion or precipitation is observed at 1000 K, as was the case for other implanted species.[1,2]

Angular scan measurement through the $\langle 100\rangle$ and $\langle 001\rangle$ crystalline direction reveal that Sb is substitutional on Ti lattice sites with $f_s \approx 0.96$ for doses up to 1×10^{15} Sb^+/cm^2 and 5×10^{15} Sb^+/cm^2, respectively. The study of room-temperature implants is limited to these doses as the damage level slowly reaches the random level. Annealing of this partially damaged rutile phase did not alter the lattice position of Sb.

Sb implantation into TiO_2 causes a large increase of the conductivity from about $10^{-13}\,\Omega^{-1}\,\mathrm{cm}^{-1}$ for the pure crystal to $31\,\Omega^{-1}\,\mathrm{cm}^{-1}$ for the high dose Sb-implanted sample. For Ar implantation the conductivity saturates with fluence at a value of about $0.3\,\Omega^{-1}\,\mathrm{cm}^{-1}$.[5] This enhancement is attributed to doping by defects, while doping by Sb contributes a further increase of the conductivity by 2 orders of magnitude. The conductivity increases very rapidly with ion fluence and approaches a saturation value. This is in agreement with results obtained after implantation of Sn where a similar conductivity saturation value of $30\,\Omega^{-1}\,\mathrm{cm}^{-1}$ was reached.[5] Comparing these results it seems that the different charge state values play a minor role for the doping mechanism. The reason why Sn and Sb cause similar doping levels, although they have different charge states, is not clear yet. Presumably compensating defects play an important role. For a Sb dose of $5\times10^{16}/\mathrm{cm}^2$ an additional increase of the conductivity is noted in the low-temperature region. It is speculated that this may be due to hopping between Sb precipitates as similar mechanisms have been noted previously for high dose Nb implants.[6]

The temperature dependence of the resistance was measured in the region between 290 and 40 K (6 K) in order to get some information on the transport mechanism. From the fact that the temperature dependence of the conductance can be described by $\ln\sigma \sim T^{-1/2}$ for the low dose samples and by $\ln\sigma \sim T^{-1/4}$ for the high dose samples, we conclude that the transport process is due to hopping, especially variable range hopping between localized states. In the theoretical description of such a transport process it is assumed that when the density of electronic states is finite and the states are localized near the Fermi energy, E_F, variable range hopping will occur and $\ln\sigma$ is then proportional to $T^{-1/4}$.[13] If in addition Coulomb repulsion between carriers is taken into account, $\ln\sigma$ is proportional to $T^{-1/2}$.[14] In the derivation of the latter dependence it is assumed that the one-electron density of states vanishes at E_F resulting in a soft Coulomb gap. For the low dose samples we conclude that the transport process is due to variable range hopping with a soft Coulomb gap near E_F, while with increasing dose the Coulomb gap is smeared out and $\ln\sigma$ is proportional to $T^{-1/4}$. The system is then nearer to the metal-semiconductor transition. A similar conclusion was drawn previously for Sn in TiO_2.[5]

The electron transport for the high dose sample is possibly due to different hopping processes which are activated in different temperature regions. Previously, hopping between precipitates of the implant and as well as of Ti have been suggested as possible transport processes in high dose implanted samples.[6]

In summary an attempt was made to study the relation between lattice site location, charge state of the implanted ion, and electrical conductivity. It turned out that the charge state does not play a big role in the doping of TiO_2 probably due to the fact that the doping centers are compensated by charged defects. The results are not yet conclusive and further systematic studies have to be performed to clarify the doping action of ions and defects in TiO_2.

ACKNOWLEDGMENTS

The authors would like to thank S. Massing for performing the ion implantation, and the Van de Graaff team for providing the analyzing He ion beam. The work was supported by the Volkswagenstiftung and the University of Jordan, Amman.

*Permanent address: University of Jordan, Amman, Jordan.
[1] R. Fromknecht, I. Khubeis, and O. Meyer, Nucl. Instrum. Methods Phys. Res. Sect. B **116**, 109 (1996), and references therein.
[2] R. Fromknecht and O. Meyer, Mater. Chem. Phys. **45**, 50 (1996).
[3] J. W. DeFord and O. W. Johnson, J. Appl. Phys. **54**, 889 (1983), and references therein.
[4] T. E. Parker and R. Kelly, J. Phys. Chem. Solids **36**, 377 (1975).
[5] R. Fromknecht, R. Auer, I. Khubeis, and O. Meyer, Nucl. Instrum. Methods Phys. Res. Sect. B (to be published).
[6] S. M. M. Ramos, B. Canut, R. Brenier, L. Gea, L. Romana, M. Brunel, and P. Thévenard, Nucl. Instrum. Methods Phys. Res. Sect. B **80/81**, 1123 (1993).
[7] J. P. Biersack and L. G. Haggmark, Nucl. Instrum. Methods **174**,257 (1980).
[8] G. P. Pells, Radiat. Eff. **64**, 71 (1982).
[9] I. Khubeis and O. Meyer, Nucl. Instrum. Methods Phys. Res. Sect. B (to be published).
[10] I. Khubeis and O. Meyer, Mater. Chem. Phys. **38**, 284 (1994).
[11] S. Nakamura, E. Yagi, T. Osaka, and M. Iwaki, Nucl. Instrum. Methods Phys. Res. Sect. B **33**, 729 (1988).
[12] S. N. Subbarao, Y. H. Yun, R. Kershaw, K. Swight, and A. Wold, Mater. Res. Bull. **13**, 1461 (1978).
[13] N. F. Mott, *Metal-Insulator Transitions* (Taylor and Francis, London, 1990).
[14] A. L. Efros and B. I. Shklovskii, J. Phys. C **8**, L49 (1975).